

Energy transfer in $\text{PbO-Bi}_2\text{O}_3\text{-Ga}_2\text{O}_3$ glasses codoped with Yb^{3+} and Er^{3+}

Luciana R. P. Kassab*

Laboratório de Vidros e Datação, Faculdade de Tecnologia de São Paulo, Centro Estadual de Educação Tecnológica Paula Souza, Praça Coronel Fernando Prestes 30, CEP 01124-060, São Paulo, São Paulo, Brazil

Marcos E. Fukumoto

Departamento de Engenharia de Sistemas Eletrônicos, Escola Politécnica da USP, Avenida Prof. Luciano Gualberto 158, Travessa R, bloco A, CEP-05508-900, São Paulo, São Paulo, Brasil

Laércio Gomes

Centro de Lasers e Aplicações, Instituto de Pesquisas Energéticas e Nucleares de São Paulo, Travessa R 400, Cidade Universitária, CEP-05508-900, São Paulo, São Paulo, Brasil

Received July 16, 2004; revised manuscript received December 28, 2004; accepted December 31, 2004

The mechanism of the $\text{Yb}^{3+} \rightarrow \text{Er}^{3+}(\text{PbO-Bi}_2\text{O}_3\text{-Ga}_2\text{O}_3)$ glasses by use of several combinations of Yb^{3+} and Er^{3+} concentrations. The measured luminescence decay curves of the donors are used to determine the experimental transfer rates; the best fittings for them are obtained with single exponentials. The microparameters are calculated and used to determine the theoretical rates. The real migration mechanism, involved in the energy transfer of each sample, diffusion, or hopping, is determined by means of the experimental transfer rates and the theoretical ones; fast excitation diffusion among donors, followed by a direct donor to acceptor energy transfer, predominates. A comparison is made with the energy-transfer mechanism of ZBLAN glass codoped with Yb^{3+} and Er^{3+} , as fast-excitation diffusion among donors, followed by direct energy transfer, was also observed. © 2005 Optical Society of America

OCIS codes: 300.2140, 160.5690.

1. INTRODUCTION

The ternary composition lead bismuth gallate ($\text{PbO-Bi}_2\text{O}_3\text{-Ga}_2\text{O}_3$), or PBG, is one of the most studied structures of the heavy metal oxide glasses.¹ These glasses are becoming an important class of materials for optoelectronics and photonics applications because of the following characteristics. They have a high refractive index (of 2.5) that produces a large transition cross section and a large optical nonlinearity with applications in photonics. They offer the advantage of high chemical stability; they can remain as long as six months in the laboratory atmosphere without visible signs of deterioration, crystallization, or hygroscopicity. The large thermal expansion coefficient ($110 \times 10^{-7} \text{ }^\circ\text{C}^{-1}$),¹ normally present in glasses with gallium, is another characteristic of PBG glasses. Low phonon energies (500 cm^{-1}), in comparison to silica, silicate, and phosphate glasses, evidenced by the extended infrared cutoff edge (up to $8 \text{ }\mu\text{m}$) are a consequence of the small field strengths and relatively large masses of the glass components.^{2,3} The principle of the forming of glass with infrared transmission to gain a longer wavelength is based on the use of compounds whose cations-anions bond is relatively weak, given a low fundamental vibration; cations with large masses are responsible for these low vibration frequencies. The low phonon energy reduces the nonradiative decay rates and provides an opportunity for the development of more effi-

cient lasers and fiber optic amplifiers at a longer wavelength than is available from other glasses as silicates ($\sim 1100 \text{ cm}^{-1}$), borates ($\sim 1400 \text{ cm}^{-1}$), germanates ($700\text{--}900 \text{ cm}^{-1}$), phosphates ($\sim 1200 \text{ cm}^{-1}$), tellurites ($500\text{--}700 \text{ cm}^{-1}$), ZBLAN ($450\text{--}560 \text{ cm}^{-1}$), and chalcogenides ($\sim 350 \text{ cm}^{-1}$).⁴ A good mechanical hardness is also another characteristic of this vitreous system.¹ In addition, as a consequence of its greater chemical resistance and greater hardness, PBG glasses may be useful for optical applications traditionally taken up by fluoride glasses.^{2,5}

The study of singly doped ($\text{PbO-Bi}_2\text{O}_3\text{-Ga}_2\text{O}_3$) glasses has already been published,^{4,6-8} but the literature presents only two studies of energy transfer in this host.^{5,9} The $^4\text{I}_{13/2} \rightarrow ^4\text{I}_{15/2}$ luminescence of Er^{3+} at $1.5 \text{ }\mu\text{m}$ has been studied for the development of a light amplifier for telecommunication devices. However, the energy level scheme does not favor the optical amplification at $1.5 \text{ }\mu\text{m}$ because of the three levels system involved. The Yb^{3+} can be an excellent sensitizer for Er^{3+} because of its broad absorption band and its high absorption cross section near 970 nm . These characteristics and the large spectral overlap between the Yb^{3+} emission and the Er^{3+} absorption result in an efficient $\text{Yb} \rightarrow \text{Er}$ energy transfer in Yb-Er codoped materials. The purpose of this work is to present, for the first time, the mechanism involved in the $\text{Yb} \rightarrow \text{Er}$ energy transfer observed in $\text{PbO-Bi}_2\text{O}_3\text{-Ga}_2\text{O}_3$

glasses produced at the Laboratory of Glasses and Data-tion. The microparameters involved are calculated and used to estimate the theoretical transfer rates predicted for a donor \rightarrow acceptor transfer assisted either by diffusion or hopping migration; then, the real mechanism of migration involved is determined by use of the theoretical values and the experimental ones. A comparison is made with Yb:Er:ZBLAN glass energy transfer mechanism.¹⁰

2. EXPERIMENT

The samples were prepared with Yb₂O₃ and Er₂O₃ added to the following glass matrix: 57.14PbO–25.11Bi₂O₃–17.75Ga₂O₃ (mol%). This composition, suggested by Dumbaugh,¹ is the most stable glass-forming composition in this system and the most stable against devitrification.^{5,9} We prepared two series of Yb:Er:PBG glasses by melting the powders in Pt crucibles at 1000 °C for 1.5 h, annealing for 3 h at 300 °C (T_g temperature is 335 °C) in heated brass molds, and then cooling inside the furnace up to room temperature. The maximum doping level that we obtained in this vitreous system was of 0.3 mol% (considering the sum Yb³⁺ and Er³⁺); higher concentration was limited by the occurrence of crystallization process and clusters that enhance the optical losses.

Polished samples with 10 \times 20 \times 2 mm³ were produced. The absorption spectra at room temperature were recorded with a spectrometer (Cary 500) in the 920–1120 nm range. The emission spectra were measured with an excitation beam of 968 nm from a AlGaAs laser diode (Optopower A020). Laser excitations were done perpendicular to the sample thickness and close to its edge to avoid reabsorption. The lifetimes of the excited ions were measured with a pulsed laser excitation (4 ns) from a tunable optical parametric oscillator pumped by the second harmonic of a Q-switched Nd-YAG laser from Quantel. Errors in these emission and fluorescence lifetime measurements are of $\pm 5\%$.

3. RESULTS

Yb \rightarrow Er energy transfer is represented in a simplified energy level diagram in Fig. 1. The lifetime of the ²F_{5/2} state of Yb³⁺ was measured for single and codoped PBG glasses; in all of the cases, the best fitting was obtained with a single exponential function. As an example we

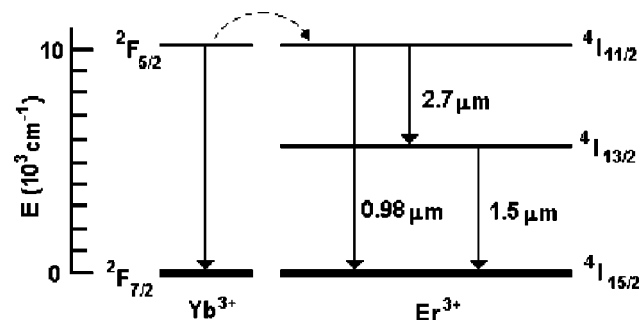


Fig. 1. Simplified energy level diagram of the ytterbium-erbium system showing radiative (solid line) and nonradiative transitions (dashed curve).

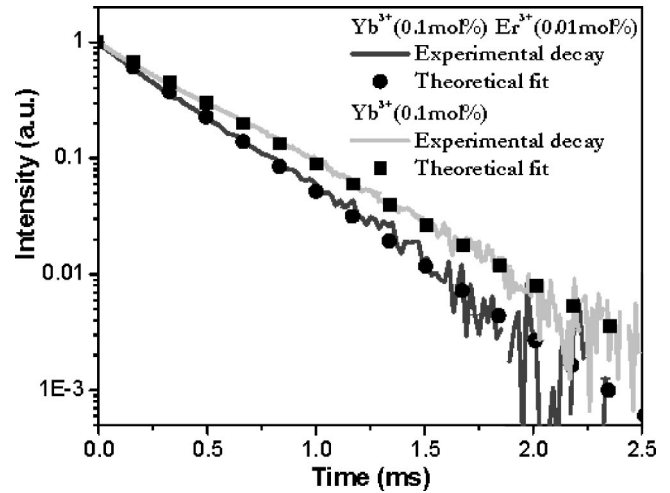


Fig. 2. Fluorescence decay of Yb³⁺ (²F_{5/2} \rightarrow ²F_{7/2}) in Yb:Er:PBG glass (0.1 mol% of Yb³⁺ and 0.01 mol% of Er³⁺) and in the Yb:PBG glass (0.1 mol% of Yb³⁺); theoretical fit and experimental results are indicated.

Table 1. Total Lifetime of the Yb³⁺ Donor in Single (τ_D) and Codoped (τ samples)^a

Yb ³⁺ (mol%)	Er ³⁺ (mol%)	τ_D ($\pm 5\%$ ms)	τ ($\pm 5\%$ ms)
0.10	0.01	0.42	0.34
0.10	0.05	0.42	0.36
0.20	0.01	0.45	0.40
0.20	0.05	0.45	0.41
0.20	0.10	0.45	0.37

^aBest fitting obtained with a single exponential function (0.1 and 0.2 mol% of Yb³⁺ represent, respectively, 2.1×10^{19} and 5.3×10^{19} ions/cm³; 0.01, 0.05, and 0.1 mol% of Er³⁺ represent, respectively, 2.2×10^{18} , 1.1×10^{19} and 2.2×10^{19} ions/cm³).

present in Fig. 2 the experimental fluorescence decay of Yb³⁺ in a codoped sample (0.1 mol% of Yb³⁺ and 0.01 mol% of Er³⁺), and in a single doped sample (0.1 mol% of Yb³⁺), and the theoretical fit for both cases. Table 1 shows the total lifetime of the donor in single and codoped samples (τ_D and τ are the total lifetime of the donor Yb³⁺ in the single and codoped samples, respectively). In Table 1, Yb³⁺ and Er³⁺ concentrations are presented in mole percent and also in ions per cubed centimeter. The microparameters (C_{D-D} and C_{D-A}) related to the energy transfer from the first and the second excited states of donors (D) to acceptors (A) were calculated with¹⁰:

$$C_{D-A} = \frac{R_{D-A}^6}{\tau_D}, \quad (1)$$

$$C_{D-D} = \frac{R_{D-D}^6}{\tau_D}. \quad (2)$$

The critical radii R_{D-D} and R_{D-A} were calculated with the equations below that use the overlap integral method based on the calculation of the emission (donor) and the absorption (acceptor or donor) cross-section superposition:

$$R_{D-D}^6 = \frac{6c\tau_D}{(2\pi)^4 n^2} \frac{g_D^{\text{low}}}{g_D^{\text{up}}} \int \sigma_{\text{emis}}^D(\lambda) \sigma_{\text{abs}}^D(\lambda) d\lambda, \quad (3)$$

$$R_{D-A}^6 = \frac{6c\tau_D}{(2\pi)^4 n^2} \frac{g_D^{\text{low}}}{g_D^{\text{up}}} \int \sigma_{\text{emis}}^D(\lambda) \sigma_{\text{abs}}^A(\lambda) d\lambda, \quad (4)$$

where c is the light speed, n is the refractive index of the medium, and g_{low}^D and g_{up}^D are the degeneracy of the respective lower and upper levels of the donor. The overlap integral was calculated with the emission (σ_{emis}^D) and absorption (σ_{abs}^D or σ_{abs}^A) cross-section superposition, respectively, calculated for D–D and D–A. The A–D back-transfer process is represented by the fraction of the initial excited Yb^{3+} ions that remains in the ${}^2\text{F}_{5/2}$ state owing to the $\text{Er}({}^4\text{I}_{11/2}) \rightarrow \text{Yb}({}^2\text{F}_{5/2})$ back-transfer process and is calculated by

$$C_{A-D} = \frac{R_{A-D}^6}{\tau_A}, \quad (5)$$

where τ_A represents the total lifetime of the acceptor state and R_{A-D} is calculated as Eq. (4) by use of the emission (σ_{emis}^A) and the absorption (σ_{abs}^D) cross-section superposition, respectively.

The emission cross section of Yb^{3+} (${}^2\text{F}_{5/2}$) was obtained from the absorption cross-section spectrum by use of the McCumber relation given by¹¹:

$$\sigma_{\text{emi}}(\lambda) = \sigma_{\text{abs}}(\lambda) \frac{Z_l}{Z_u} \exp\left(\frac{E_{z_l} - hc\lambda^{-1}}{kT}\right), \quad (6)$$

where k and E_{z_l} represent the Boltzman's constant and the zero-line energy that is defined as the energy separation between the lowest components of the upper and lower states, respectively. E_{z_l} is associated with the most intense peak in the absorption spectrum of Yb^{3+} doped glass; in the high-temperature limit, the ratio of the partition functions (Z_l/Z_u) simply becomes the degeneracy weighting of the two states.

As example we present in Fig. 3 the spectra superposition between the Yb^{3+} emission (${}^2\text{F}_{5/2} \rightarrow {}^2\text{F}_{7/2}$) and the Er^{3+} absorption (${}^4\text{I}_{15/2} \rightarrow {}^4\text{I}_{11/2}$) cross sections in $\text{Yb}:\text{Er}:\text{PBG}$ glass (0.1 mol% of Yb^{3+} and 0.01 mol% of Er^{3+}); the

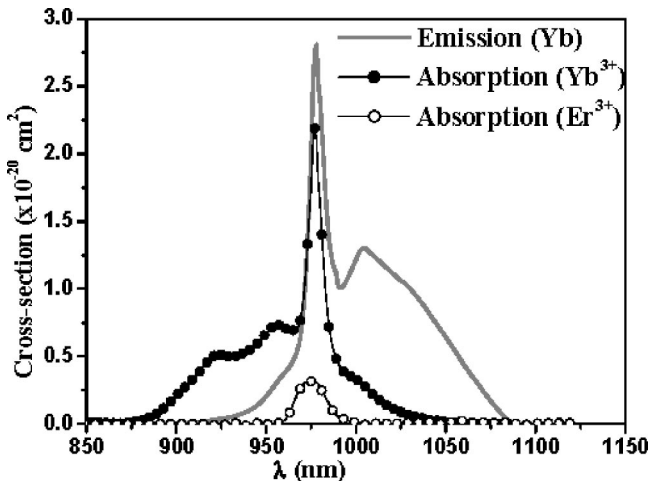


Fig. 3. Spectra superposition between the Yb^{3+} emission (${}^2\text{F}_{5/2} \rightarrow {}^2\text{F}_{7/2}$) and the Er^{3+} absorption (${}^4\text{I}_{15/2} \rightarrow {}^4\text{I}_{11/2}$) cross sections in $\text{Yb}:\text{Er}:\text{PBG}$ glass (0.1 mol% of Yb^{3+} and 0.01 mol% of Er^{3+}); absorption cross section of Yb^{3+} in PBG glass is also presented (0.1 mol% of Yb^{3+}).

absorption cross section of Yb^{3+} in PBG glass is also presented (0.1 mol% of Yb^{3+}). The strong observed spectral superposition indicates a resonant and efficient energy transfer from Yb^{3+} (${}^2\text{F}_{5/2}$) to Er^{3+} (${}^4\text{I}_{11/2}$) in PBG glass. The values obtained for the microparameters and critical radii are

$$\text{Yb}({}^2\text{F}_{5/2}) \rightarrow \text{Yb}({}^2\text{F}_{5/2}),$$

$$C_{D-D} = (108 \pm 12) \times 10^{-40} \text{ cm}^6 \text{ s}^{-1}, \quad R_{D-D} = 12.92 \text{ \AA},$$

$$\text{Yb}({}^2\text{F}_{5/2}) \rightarrow \text{Er}({}^4\text{I}_{11/2}),$$

$$C_{D-A} = (18 \pm 2) \times 10^{-40} \text{ cm}^6 \text{ s}^{-1}, \quad R_{D-A} = 9.60 \text{ \AA}.$$

The fact that $C_{D-D} \approx 6C_{D-A}$ indicates that the excitation migration among Yb^{3+} ions must be an important effect in the $\text{Yb} \rightarrow \text{Er}$ energy transfer in PBG glass. For ZBLAN glass¹⁰ this value is $C_{D-D} \approx 3.8C_{D-A}$, as $C_{D-D} = 67.7 \times 10^{-40} \text{ cm}^6 \text{ s}^{-1}$ and $C_{D-A} = 17.6 \times 10^{-40} \text{ cm}^6 \text{ s}^{-1}$.

The differences between C_{D-A} and C_{D-D} parameters, considering PBG and ZBLAN glasses, are explained by Eqs. (3) and (4). For example, in the case of $\text{Yb}:\text{Er}:\text{PBG}$, the emission and the absorption cross sections, at 977 nm, are $2.8 \times 10^{-20} \text{ cm}^2$ and $2.3 \times 10^{-20} \text{ cm}^2$, respectively, whereas for $\text{Yb}:\text{Er}:\text{ZBLAN}$ these values are $1.0 \times 10^{-20} \text{ cm}^2$ and $0.8 \times 10^{-20} \text{ cm}^2$, respectively.

The donor fluorescence decay in the presence of the acceptor was analyzed with current models found in the literature that consider the excitation migration between donors. In this model a multistep transfer process occurs; the excitation energy, described as a quasi particle migrating on a lattice (localized exciton with electron and hole, both located at the same ion and moving together as a Frenkel exciton¹²), and transferred from an activator to another several times, is followed by the occurrence of the final transfer to an acceptor. The mathematical description is the one used for the exciton migration. To determine the real mechanism of migration, diffusion or hopping, we must calculate the theoretical parameters (k_d and k_h) and the experimental one (k). The $D \rightarrow A$ energy transfer k_d involving diffusion can be calculated from the multistep energy transfer, treating the diffusion between donors like a random walk, using the following equation¹³:

$$k_d = 21c_A c_D (C_{D-D}^3 C_{D-A})^{1/4}, \quad (7)$$

where c_A and c_D are the donor and acceptor concentrations. In this model, it is assumed that an excitation created at time $t=0$, within the trapping radius, has an infinite trapping rate.

Another approach is the hopping model, which can be applied to describe the incoherent excitation migration between donor states by use of the average hopping time t_h , i.e., the excitation will be scattered at each step in the random walk. If a trapping radius is defined as the distance at which the rate of donor–acceptor transfer is equal to the hopping rate, the overall energy transfer rate becomes¹⁴:

$$k_h = 20c_A c_D (C_{D-D} C_{D-A})^{1/2}. \quad (8)$$

Table 2 presents the theoretical (k_d) and experimental (k) transfer parameters for all of the codoped samples produced. The experimental transfer rates (k) are calculated with the following expression:

$$k = \frac{1}{A\tau} - \frac{1}{A\tau_D}, \quad (9)$$

where $A = 1 - B$, represents the fraction of Yb^{3+} that interacts with Er^{3+} and $B = C_{A-D}/(C_{A-D} + C_{D-A})$ is associated with the back-transfer process; in our case $C_{A-D} = 15 \times 10^{-40} \text{ cm}^6 \text{ s}^{-1}$, $B = 0.46$, and $A = 0.54$. So the fraction of Yb^{3+} that interacts with Er^{3+} is more than 50%. A similar back-transfer process¹⁰ occurs for Yb:Er:ZBLAN , as $C_{A-D} = 12 \times 10^{-40} \text{ cm}^6 \text{ s}^{-1}$, and the fraction of Yb^{3+} that interacts with Er^{3+} is 70%.

The criterion to find the real excitation migration mechanism was presented recently in the literature¹³ as it is used in this paper, in Section 4. It is based on defining $R = k/k_d$. For $R = 1$ or $k = k_d$ the excitation migration is assisted by diffusion and for $R > 1$ or $k > k_d$, it is composed by fast excitation diffusion among donors followed by the direct energy transfer. For $R < 1$ or $k < k_d$ the excitation migration is assisted by hopping.

4. DISCUSSION

From Table 1 we notice that the donor fluorescence lifetime (τ_D) is not strongly modified by the presence of the acceptor. The fluorescence lifetime in the single doped samples (τ_D) almost does not change and indicates no transfer of energy to impurities, OH, etc. The variations of the fluorescence lifetime in the codoped samples (τ) are more significant and are associated with the $\text{Yb}^{3+} \rightarrow \text{Er}^{3+}$ energy transfer. For 0.2 mol% of Yb^{3+} the fluorescence lifetime (τ) tends to decrease with the increase of the acceptor concentration. These facts explain the variations of the k parameter, in Table 2, as it depends on the values of τ_D and τ [Eq. (9)]. The results presented in Table 2 show that, for all the cases $k > k_d$ (or $R > 1$) and fast-excitation diffusion among donors followed by direct donor to acceptor, energy transfer predominates; energy transfer, assisted only by diffusion among donors, is not observed because in any of the cases $k = k_d$. A fast-excitation diffusion among donors was also observed for a Yb:Er:ZBLAN energy transfer.¹⁰

The largest value for the experimental transfer rate ($k = 1037.5 \text{ s}^{-1}$, in Table 2) is obtained for the sample with 0.1 mol% of Yb^{3+} and 0.01 mol% of Er^{3+} , followed by the one with 0.2 mol% of Yb^{3+} and 0.1 mol% of Er^{3+} ($k = 889.2 \text{ s}^{-1}$). For these cases fast-excitation migration occurs in the two shortest times (0.96 and 1.12 ms, respectively). For Yb:Er:ZBLAN ¹⁰ this process, for low doping levels of Yb^{3+} ($< 1 \text{ mol}\%$), occurs in significantly shorter time, about 0.05 ms.

The results of the equation below [Eq. (10)] confirm the conclusions above and are shown in Table 3. Equation (10) calculates the efficiency of the fast-excitation diffusion among donors followed by the direct energy transfer based on the competition between this process (repre-

Table 2. Theoretical (k_d) and Experimental (k) Transfer Parameters for Yb:Er:PBG Glasses^a

Yb^{3+} (mol%)	Er^{3+} (mol%)	k_d (s^{-1})	k (s^{-1})	$R = k/k_d$
0.10	0.01	8.92	1037.5	116.3
0.10	0.05	44.61	734.9	16.5
0.20	0.01	22.31	514.4	23.1
0.20	0.05	111.53	401.5	3.6
0.20	0.10	223.07	889.8	4.0

^a R gives the character of the real donor migration mechanism.

Table 3. Calculated Efficiency of the ET1 Process (eff1) in Yb:Er:PBG Glasses

Yb^{3+} (mol%)	Er^{3+} (mol%)	γ_{theor}	eff(1)
0.10	0.01	0.80	0.99
0.10	0.05	4.00	0.93
0.20	0.01	0.80	0.96
0.20	0.05	4.00	0.76
0.20	0.10	7.00	0.77

sented by $\text{ET1} = k$) and diffusion-assisted energy transfer [represented by $\text{ET2} = \gamma(\text{theor})^2 + k_d$]. The efficiency of ET1 is calculated as follows¹⁰:

$$\text{eff}(1) = \frac{k}{k + \gamma(\text{theor})^2 + k_d}, \quad (10)$$

where

$$\gamma(\text{theor}) = \left[\frac{4}{3} \pi^{(3/2)} \right] c_A (C_{D-A})^{(1/2)}. \quad (11)$$

The results of Table 3 indicate that ET1 dominates the $D \rightarrow A$ energy transfer for all the cases. For Yb:Er:ZBLAN glass, the same applies, as ET1 always dominates the $D \rightarrow A$ energy transfer.¹⁰ However the efficiency is 0.90 for larger concentration of Yb^{3+} ($> 5.0 \text{ mol}\%$). In our case, even for small concentration of Yb^{3+} (0.1 and 0.2 mol%) the efficiency is larger than 0.90 (Table 3). For a fixed doping level of Yb^{3+} , the efficiency tends to decrease, whereas the concentration of Er^{3+} increases. This fact indicates that the fast-excitation diffusion is influenced by the acceptor concentration, as also observed in Yb:Er:ZBLAN glass.¹⁰

The maximum doping level in this vitreous system is low if compared with phosphates, fluorides, and silicates. However, we have to note that this fact does not limit the applications: With long interaction lengths, fiber laser applications do not always require bulk-laser-like dopant concentrations. Besides, concerning the transfer mechanism studied in our paper, we observe that the efficiency of the process in PBG glass is high for the low doping level of the donor.

We can also corroborate the prediction of da Vila *et al.*¹⁰ that states that the fast-diffusion effects observed for Yb-Er energy transfer in ZBLAN may be present in any other resonant $D \rightarrow A$ energy transfer with a microscope donor-donor transfer constant $C_{D-D} > 67.7 \times 10^{-40} \text{ cm}^6 \text{ s}^{-1}$.

Moreover, when the energy-transfer efficiency is reduced by back transfers from the activators (acceptors) to the sensitizers (donors), the migration may favor the transfer sensitizer→activator compared with the back transfer because of the relative concentrations of the codopants ($c_D > c_A$), as observed in Table 3.

Finally, the authors think that the criterion proposed in Ref. 13 and its use in this paper represent a contribution for identifying the migration mechanism involved in the energy transfer, because the current models found in the current literature do not allow the identification when fast-excitation diffusion among donors followed by the direct energy transfer is occurring. Our criterion is that, in this case, one must observe $R > 1$.

5. CONCLUSION

In this work, PbO–Bi₂O₃–Ga₂O₃ glasses codoped with different concentrations of Yb³⁺ and Er³⁺ are studied for the first time. The mechanism of energy transfer observed is fast-excitation migration assisted by diffusion among donors, followed by direct donor–acceptor energy transfer. Even for low donor concentrations (0.1 and 0.2 mol%), the efficiency of the fast diffusion is high (>0.9). The sample with 0.1 mol% of Yb³⁺ and 0.01 mol% of Er³⁺ exhibits the largest experimental energy-transfer rate and the shortest time (0.96 ms) for the fast-excitation migration; a back-transfer process is evaluated and competes with the process of energy transfer.

ACKNOWLEDGMENT

We thank Coordenação de Aperfeiçoamento de Pessoal de Nível Superior, Instituto de Física da Universidade de São Paulo, and Laboratório de Sistemas Integráveis da Escola Politécnica da Universidade de São Paulo.

*Corresponding author; e-mail: kassablm@osite.com.br.

REFERENCES

1. W. H. Dumbaugh, "Heavy metal oxide glasses containing Bi₂O₃," *Phys. Chem.* **27**, 119–122 (1986).
2. D. Lezal, J. Pedlikova, P. Kostka, J. Bludska, M. Poulain, and J. Zavadil, "Heavy metal oxide glasses: preparation and physical properties," *J. Non-Cryst. Solids* **284**, 288–295 (2001).
3. W. H. Dumbaugh, "Lead bismuthate glasses," *Phys. Chem. Glasses* **19**, 121–125 (1978).
4. Y. G. Choi and J. Heo, "1.3 μm emission and multiphonon relaxation phenomena in PbO–Bi₂O₃–Ga₂O₃ glasses doped with rare-earths," *J. Non-Cryst. Solids* **217**, 199–207 (1997).
5. D. J. Coleman, S. D. Jackson, P. Golding, and T. King, "Measurements of the spectroscopic and energy transfer parameters for Er³⁺ doped and Er³⁺, Pr³⁺ codoped PbO–Bi₂O₃–Ga₂O₃ glasses," *J. Opt. Soc. Am. B* **19**, 2927–2937 (2002).
6. J. Heo, Y. B. Shin, and J. N. Jang, "Spectroscopic analysis of Tm³⁺ in PbO–Bi₂O₃–Ga₂O₃ glass," *Appl. Opt.* **34**, 4284–4289 (1995).
7. L. R. P. Kassab, L. C. Courrol, A. S. Morais, C. M. S. P. Mendes, S. H. Tatum, N. U. Wetter, and L. Gomes, "Spectroscopic properties of lead fluoroborate and heavy metal oxide glasses doped with Yb³⁺," *J. Non-Cryst. Solids* **304**, 233–237 (2002).
8. L. R. P. Kassab, S. H. Tatum, A. S. Morais, L. C. Courrol, N. U. Wetter, and V. L. R. Salvador, "Optical properties of Nd doped Bi₂O₃–PbO–Ga₂O₃ glasses," *Opt. Express* **6**, 104–108 (2000).
9. Y. B. Shin, H. T. Lim, Y. G. Choi, Y. S. Kim, and J. Heo, "2.0 μm emission properties and energy transfer between Ho³⁺ and Tm³⁺ in PbO–Bi₂O₃–Ga₂O₃ glasses," *J. Am. Ceram. Soc.* **83**, 787–791 (2000).
10. L. D. da Vila, L. Gomes, L. V. G. Tarelho, S. J. L. Ribeiro, and Y. Messadeq, "Mechanism of the Yb–Er energy transfer in fluorozirconate glass," *J. Appl. Phys.* **93**, 1–8 (2003).
11. D. E. McCumber, "Einstein relations connection broadband emission and absorption spectra," *Phys. Rev.* **136**, 954–957 (1964).
12. R. C. Powell, *Physics of Solid State Laser Material* (Springer, New York, 1998), Chap. 5.
13. F. H. Jagosich, L. Gomes, L. V. G. Tarelho, L. C. Courrol, I. M. Ranieri, "Deactivation effects of the lowest excited states of Er³⁺ and Ho³⁺ introduced by Nd³⁺ ions in LiYF crystals," *J. Appl. Phys.* **91**, 624–632 (2002).
14. R. K. Watts, *Optical Properties of Ions in Solids* (Plenum, New York, 1975), pp. 307.